Journal of Biomechanics 77 (2018) 91–98

Contents lists available at ScienceDirect

Journal of Biomechanics

journal homepage: www.elsevier.com/locate/jbiomech
www.JBiomech.com

# Development of a preclinical natural porcine knee simulation model for the tribological assessment of osteochondral grafts *in vitro*

P. Bowland, E. Ingham, J. Fisher, L.M. Jennings *

*Institute of Medical & Biological Engineering, School of Mechanical Engineering, University of Leeds, Leeds, UK*

ARTICLE INFO

*Article history:*
Accepted 19 June 2018

*Keywords:*
Tribology
Joint simulator
Natural knee joint
Osteochondral graft
Allograft
Cartilage
Alicona
Wear analysis

ABSTRACT

In order to pre-clinically evaluate the performance and efficacy of novel osteochondral interventions, physiological and clinically relevant whole joint simulation models, capable of reproducing the complex loading and motions experienced in the natural knee environment are required. The aim of this study was to develop a method for the assessment of tribological performance of osteochondral grafts within an *in vitro* whole natural joint simulation model.

The study assessed the effects of osteochondral allograft implantation (existing surgical intervention for the repair of osteochondral defects) on the wear, deformation and damage of the opposing articular surfaces. Tribological performance of osteochondral grafts was compared to the natural joint (negative control), an injury model (focal cartilage defects) and stainless steel pins (positive controls). A recently developed method using an optical profiler (Alicona Infinite Focus G5, Alicona Imaging GmbH, Austria) was used to quantify and characterise the wear, deformation and damage occurring on the opposing articular surfaces. Allografts inserted flush with the cartilage surface had the lowest levels of wear, deformation and damage following the 2 h test; increased levels of wear, deformation and damage were observed when allografts and stainless steel pins were inserted proud of the articular surface. The method developed will be applied in future studies to assess the tribological performance of novel early stage osteochondral interventions prior to *in vivo* studies, investigate variation in surgical precision and aid in the development of stratified interventions for the patient population.

© 2018 The Author(s). Published by Elsevier Ltd. This is an open access article under the CC BY license (http://creativecommons.org/licenses/by/4.0/).

## 1. Introduction

There is an increasing clinical need for effective early intervention osteochondral therapies that can restore the structure and function of cartilage and bone tissue. The complex biphasic structure and composition of cartilage provides exceptional functional properties allowing low friction movement under high load bearing conditions. The limitations in current therapies have prompted widespread research in the field of tissue engineering to develop alternative treatment strategies. Tissue engineered osteochondral scaffolds and constructs have the potential to regenerate cartilage and bone tissues that possess the structural, biological, mechanical and tribological properties of native cartilage and bone (Bowland et al., 2015).

The development of such early stage repair interventions in the knee, requires an understanding of how the range of variables in the natural knee environment interact with the design and material properties of the intervention to determine mechanical and tribological performance (Liu et al., 2015). Whole joint experimental simulation models, capable of reproducing the complex physiological loading, motions and interactions in the natural knee, can play a key role in the preclinical testing of early osteochondral interventions in order to determine mechanical and tribological performance prior to *in vivo* studies.

Although it is recognised that ultimately pre-clinical testing should be performed using human cadaveric tissue, the use of animal tissue can be extremely useful for methodology development. The porcine knee joint is particularly suitable as an osteochondral repair model for the following reasons: Joint size, loading, cartilage and trabecular bone thickness that more closely match the human condition than alternative animal models (Chu et al., 2010); easily obtainable from commercial suppliers, where sufficient numbers of samples can be obtained from animals slaughtered at a uniform age and of good health; lower levels of inter-specimen variability and good cartilage and bone quality when compared with donor human tissue; and finally the absence of age related changes and degeneration in porcine cartilage and bone tissue may be more representative of general tissue quality in the younger population

* Corresponding author at: Institute of Medical & Biological Engineering, School of Mechanical Engineering, University of Leeds, Leeds LS2 9JT, UK.
*E-mail address:* l.m.jennings@leeds.ac.uk (L.M. Jennings).

https://doi.org/10.1016/j.jbiomech.2018.06.014
0021-9290/© 2018 The Author(s). Published by Elsevier Ltd.
This is an open access article under the CC BY license (http://creativecommons.org/licenses/by/4.0/).

in which early intervention therapies are the most clinically relevant.

Currently, there are no published studies reporting the development of an *in vitro* whole joint simulation model, capable of the preclinical tribological assessment of early osteochondral repair interventions. A tribological whole natural porcine tibiofemoral knee joint simulation model has been previously validated and described by Liu et al. (2015). The overall aim of this study was to extend the method developed by Liu et al. (2015) to be able to assess the tribological performance (in terms of wear, deformation and damage) of osteochondral grafts within the *in vitro* whole natural joint simulation model of the porcine tibiofemoral joint. Specifically the aim was to develop a method that showed quantifiable wear, deformation and damage on the opposing surface to the intervention for a positive control osteochondral graft (metal pin) and then apply the method to quantify the resulting wear, deformation and damage on the opposing surface as a result of allograft implantations and focal cartilage defects, and begin to explore the effects of surgical precision in graft implantation on tribological performance through the assessment of proud grafts.

## 2. Materials and methods

### 2.1. Study design

A full description of the experimental groups is provided in Table 1 and an overview shown in Fig. 1. All experimental group samples (n = 4 for each group) were tested in the single station knee simulator for a duration of 7200 cycles at 1 Hz (2 h) in a lubricant of 25% (v/v) newborn calf serum (Gibco Life Technologies, Paisley, UK) in PBS.

### 2.2. Porcine knee joint preparation

Porcine tibiofemoral joints were obtained from the right hind legs of pigs aged 4–6 months old within 24 hrs of slaughter. The porcine tibiofemoral joints were braced in their natural physiological alignment, all tissue and ligaments were dissected away, leaving the meniscus *in situ*.

The centre of rotation of the femoral condyles was determined using a templating methodology (McCann et al., 2008). The femur and tibia were cemented (polymethylmethacrylate (PMMA) cement; WHW plastics, UK) and aligned in custom built test pots, using a purpose built mounting rig that replicated the internal working heights and orientation of the simulator. The axial force was offset 7% of the width of the porcine joint in a medial direction from the tibial axis to ensure more medial loading. The braces were then removed from the tibiofemoral joint and the porcine sample was mounted within a gaiter (holding lubricant) in the natural knee simulator.

**Table 1**
Description of the experimental groups (n = 4 per group). All experimental tests run for 7200 cycles at 1 Hz (2 h) in the single station knee simulator.

| Experimental Group | Description |
|---|---|
| Negative Control | Articulating surfaces intact (native state). |
| Cartilage Defects | 6 mm diameter cartilage defect to subchondral bone. |
| Allografts Flush | 6 mm diameter porcine osteochondral graft inserted flush with cartilage surface. |
| Allografts 1 mm Proud | 6 mm diameter porcine osteochondral graft inserted 1 mm proud of cartilage surface. |
| Stainless Steel Pins Flush (Positive Control 1) | 6 mm diameter stainless steel pin inserted flush with cartilage surface. |
| Stainless Steel Pins 1 mm Proud (Positive Control 2) | 6 mm diameter stainless steel pin inserted 1 mm proud of cartilage surface. |

Osteochondral allografts were harvested using a 6 mm diameter drill aided corer from the contact area of porcine medial femoral condyles. Acufex™ (Smith & Nephew, USA) mosaicplasty surgical drill attachment, drill guide and delivery tamp tools were used for the creation of recipient donor sites and the subsequent implantation of osteochondral allografts and stainless steel pins. Full thickness cartilage defects were created using a 6 mm diameter biopsy punch with the defect extending down to the subchondral bone. For the 1 mm proud grafts, these were 1 mm longer than the standard (flush) grafts, and the implantation procedure was identical (implant hole depth same for all groups). Tissue samples were kept hydrated throughout the preparation procedures using phosphate buffered saline (PBS; MP Biomedicals LLC, UK) and stored until required for testing on PBS soaked tissue paper at −20 °C. Samples were removed from storage prior to testing and thawed at room temperature.

### 2.3. Single station natural knee simulator

The methods presented in this study were developed from the simulation model as described by Liu et al. (2015). The ProSim electromechanical single station natural knee simulator (Simulation Solutions, Manchester, UK) was used with a standard gait kinematic input profile, which scaled the high kinematic Leeds knee input profiles (McEwen et al., 2005) to the kinematic limits of porcine knee tissue. The simulator had six degrees of freedom and five axis of controlled motion. The axial load (AF) was force controlled; flexion-extension (FE) and tibial rotation (TR) were displacement controlled; the medial-lateral axis was fully constrained; and abduction-adduction (AA) was not controlled and left unconstrained (passive motion). Anterior-posterior (AP) displacement was not driven and was constrained through the use of springs (k = 2.69 $N.mm^{-1}$). The spring constraints were used to replicate ligament function and achieve rolling and sliding motions of the femur relative to the tibia.

The kinematic input profile applied a peak axial load of 1000 N, a flexion-extension range of 0–21° and tibial rotation of 1.6–1.6° at a frequency of 1 Hz. AP displacement and AP shear force data were recorded for each test. The AP shear force was the force transmitted from the femur to tibia along the AP axis and was used as a measure of friction occurring between the articulating surfaces of the tibiofemoral joint (Liu et al., 2015).

All porcine knees, excluding the negative control, were initially run for 900 cycles at 1 Hz as a reference test to check stability and that each sample could reproduce the AP shear force and displacement outputs demonstrated during the full negative control group tests (7200 cycles at 1 Hz). The porcine knees were then removed from the simulator and allowed to recover for 1 h before either a 6 mm diameter allograft, cartilage defect or stainless steel pin was inserted into the centre of the contact area on the medial femoral condyle. The samples were then mounted back into the simulator and run as the experimental group tests (Table 1) (7200 cycles at 1 Hz).

### 2.4. Assessment and quantification of articular surface wear, deformation and damage

The surface wear, deformation and damage present on the opposing meniscal surfaces to the medial femoral condyle was assessed and quantified using an Alicona Infinite Focus G5 optical profiler. The Alicona Infinite Focus is an optical device for 3D surface measurement and analysis which operates using focus variation technology. Focus variation combines the small depth of focus of an optical system with vertical scanning in order to provide topographical and full colour information from the variation of focus. The system (Fig. 2) consists of a movable XY-stage above

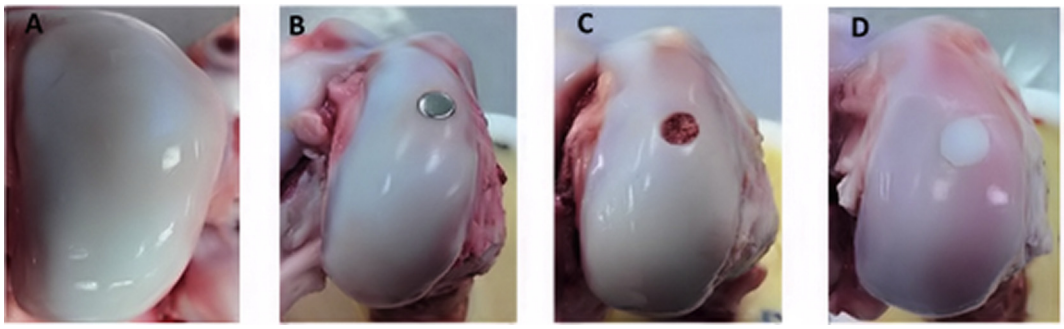


**Fig. 1.** Overview of experimental groups (images of medial femoral condyles). (A) Negative control group (native state); (B) Positive control groups 1 & 2 (stainless steel pins inserted flush or 1 mm proud); (C) Cartilage Defects; (D) Allografts flush and 1 mm proud groups.

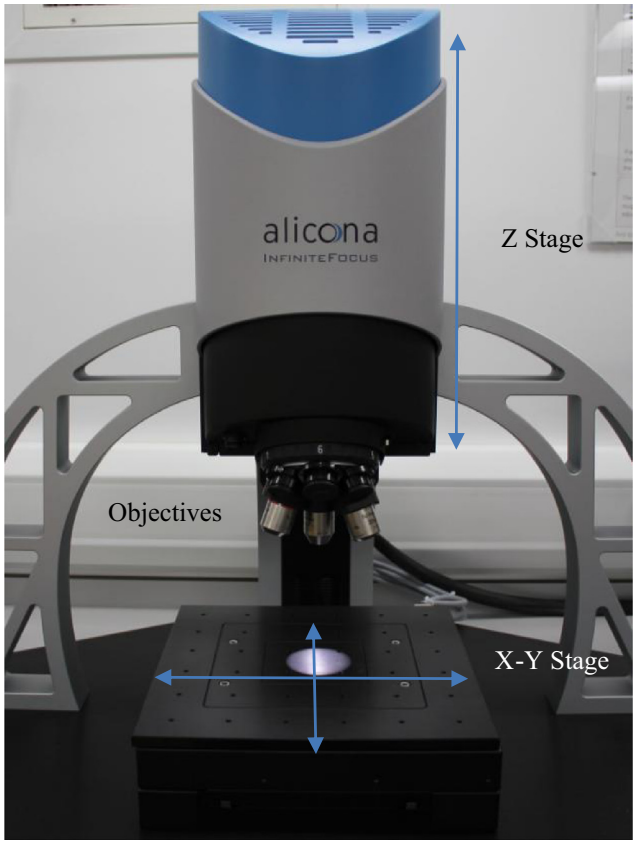


**Fig. 2.** The Alicona Infinite Focus G5 optical profiler used for the determination of change of volume of the opposing meniscal surface.

which the objectives (5x, 10x & 20x) are mounted on a rotating turret. The medial meniscal surfaces were replicated with Accutrans AB (Coltene Whaledorf AG, Switzerland) brown casting silicone; replication enables high resolution optical metrology of hard-to-measure surfaces. The use of replication material and the Alicona optical profiler to determine volume change of cartilage has been validated by Bowland (2016). The silicon replicas were scanned on the Alicona Infinite Focus using a 10x objective, 213 nm vertical resolution and 3.91 μm lateral resolution to produce 3D image datasets of the original meniscal surface.

The volume ($mm^3$) extending below the meniscal surface (Fig. 3) was measured for all experimental groups; this value was used as a measure of the level of wear, deformation and damage occurring during simulator testing due to the presence of focal cartilage defects (injury model), allografts (intervention) and stainless steel pins (positive control) in the medial femoral condyles. It was not possible to assume that changes in surface geometry (increase in measured volume extending below the meniscal surface) were solely due to wear arising from removal of material/tissue, changes in surface geometry may also have been attributable to tissue damage and deformation without the loss of material.

The mean penetration depth of wear, deformation and damage occurring on the meniscal surfaces was also quantified (not applicable for negative control group). All parameters were measured from the 3D image datasets, using the analysis software IF Measure Suite Version 5.1 (Alicona, Austria).

One way analysis of variance ($p < 0.05$ significance level) with a Games-Howell post hoc test was used to determine significant differences in both mean volume extending below the meniscal surface and penetration depth between the experimental groups. Data was plotted as the mean ($n = 4$) ±95% confidence intervals. The data associated with this article are openly available from the University of Leeds Data Repository (Bowland et al., 2018).

## 3. Results

### 3.1. AP shear force and displacement

At the end of testing (time point 120 min), the mean AP shear force (Fig. 4) and AP displacement (Fig. 5) were similar for all groups with the exception of the allograft 1 mm proud group, which appeared to have a different offset for both AP shear force and AP displacement.

### 3.2. Articular cartilage surface wear, deformation and damage

Wear, deformation and damage present on the opposing articulating surfaces following the experimental simulation was confined to the central region of the medial meniscus, due to the meniscus covering the large majority of the tibial plateau. No visible damage, wear or deformation was present on the meniscal surfaces of the negative control samples; the mean volume extending below the surface of the negative control samples was < 0.1 $mm^3$.

Wear, deformation and damage was most severe in positive control group 2 (stainless steel pins 1 mm proud) comprising of deep circular lesions at the most posterior point of AP displacement, followed by a defined sweeping lesion up towards the anterior edge of the meniscus (Fig. 6E). Damage, wear and deformation patterns were similar in positive control group 1 (stainless steel pins flush) but were less pronounced (Fig. 6D).

Positive control groups 1 and 2 had the largest mean volumes extending below the surface at 3.54 $mm^3$ and 20.89 $mm^3$ respectively, reflecting the high levels of surface damage, wear

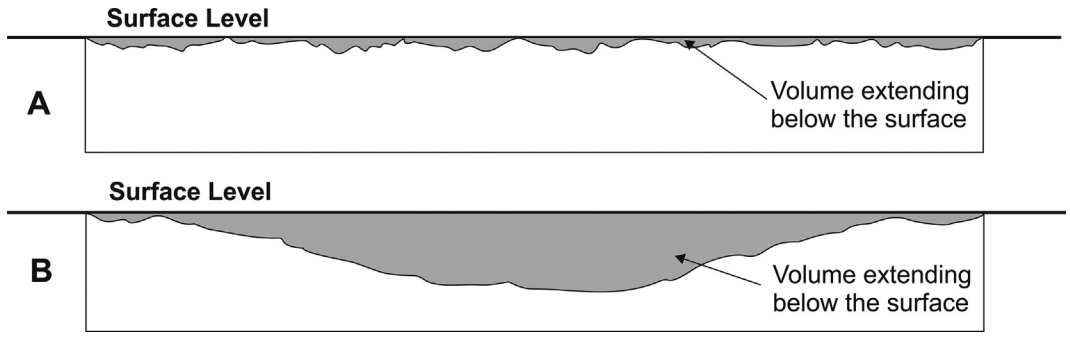


**Fig. 3.** Schematic diagram representing the volume extending below the meniscal surface as measured by the Alicona. (A) Untested sample; (B) Post-test sample with changes in surface geometry due to damage, wear and deformation.

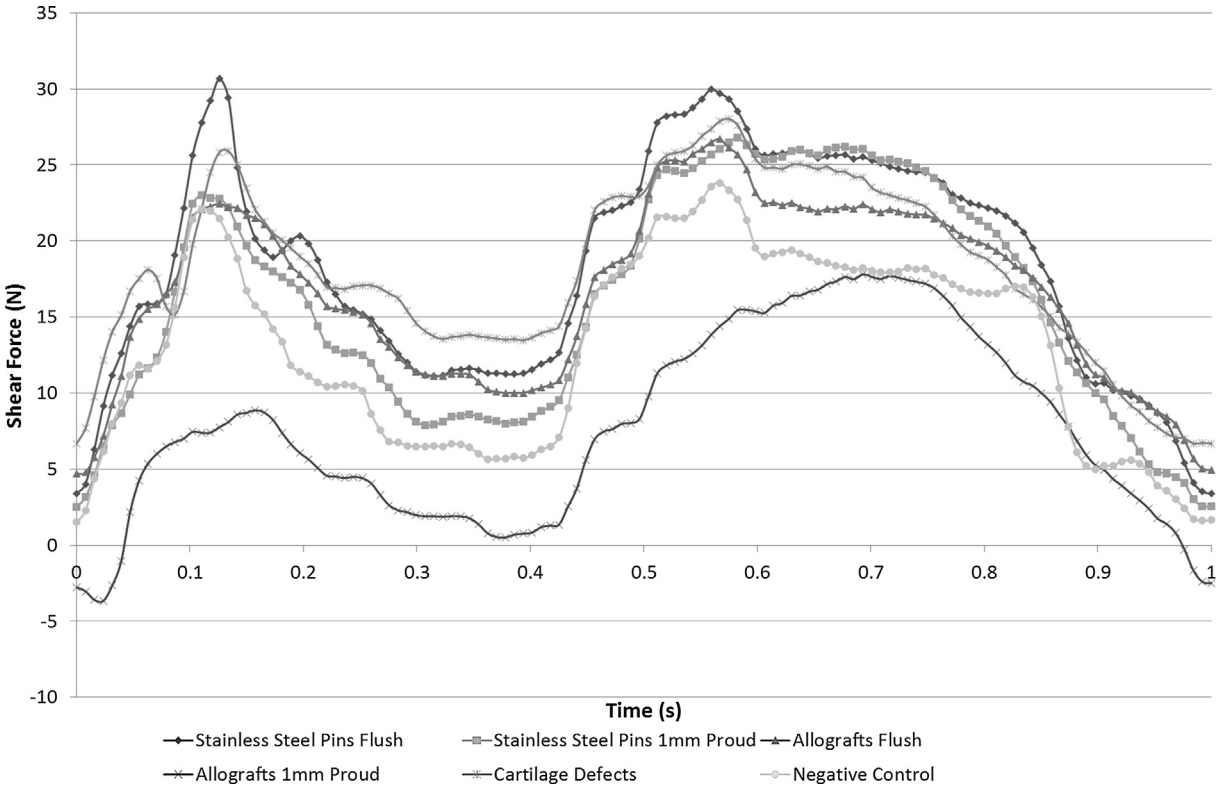


**Fig. 4.** Mean shear force values at 120 min test duration plotted against time during one cycle (1s) of the gait cycle (n = 4).

and deformation (Fig. 7). The mean volume of positive control group 2 was significantly ($p < 0.01$) greater than the negative control group. However there was no significant difference between positive control group 1 and the negative control ($p > 0.12$) likely due to the high variation seen in positive control group 1 ($3.54 \pm 1.38\ mm^3$). This variation was attributable to one outlier with a low volume at $1.06\ mm^3$.

The allograft flush group had the lowest mean volume at $0.17\ mm^3$; similarly, the cartilage defect group was also low at $0.26\ mm^3$ when compared to the allograft 1 mm proud ($0.46\ mm^3$) and positive control groups. The volume extending beneath the surface of the cartilage defect ($p = 0.222$) and allograft flush ($p = 0.401$) groups was not significantly different when compared to the negative control group. Similarly, no significant difference ($p = 0.766$) was present between the cartilage defect and allograft flush group. Damage, wear and deformation present on the meniscal surfaces of the allograft flush and cartilage defect group consisted predominantly of long scratches parallel with the axis of AP motion (Fig. 6A & C). Two samples within the cartilage defect group had circular extrusions (approximately 6 mm in diameter and 60 μm in height) present on the surface of the meniscus at the most posterior point of AP displacement (Fig. 6C).

Wear, deformation and damage in the allograft 1 mm proud group also consisted of long scratches orientated parallel with the AP axis (Fig. 6B), however, the scratches were visibly wider and deeper within this group. The majority of allograft 1 mm proud samples also had hemispherical depressions in the meniscal tissue surface with a maximum diameter of 6 mm; these depressions were located at the most posterior point of AP displacement on the meniscal surface (Fig. 6B). Damage or wear to the meniscal tissue was not visible in the regions of the hemispherical depressions.

Penetration depth (Fig. 8) was greatest in the stainless steel pins inserted 1 mm proud group (0.58 mm) and was significantly different ($p = 0.008$) to stainless steel pins inserted flush (0.38 mm). Allografts inserted 1 mm proud also had a greater mean penetration depth (0.015 mm) to their flush counterparts (allografts flush;

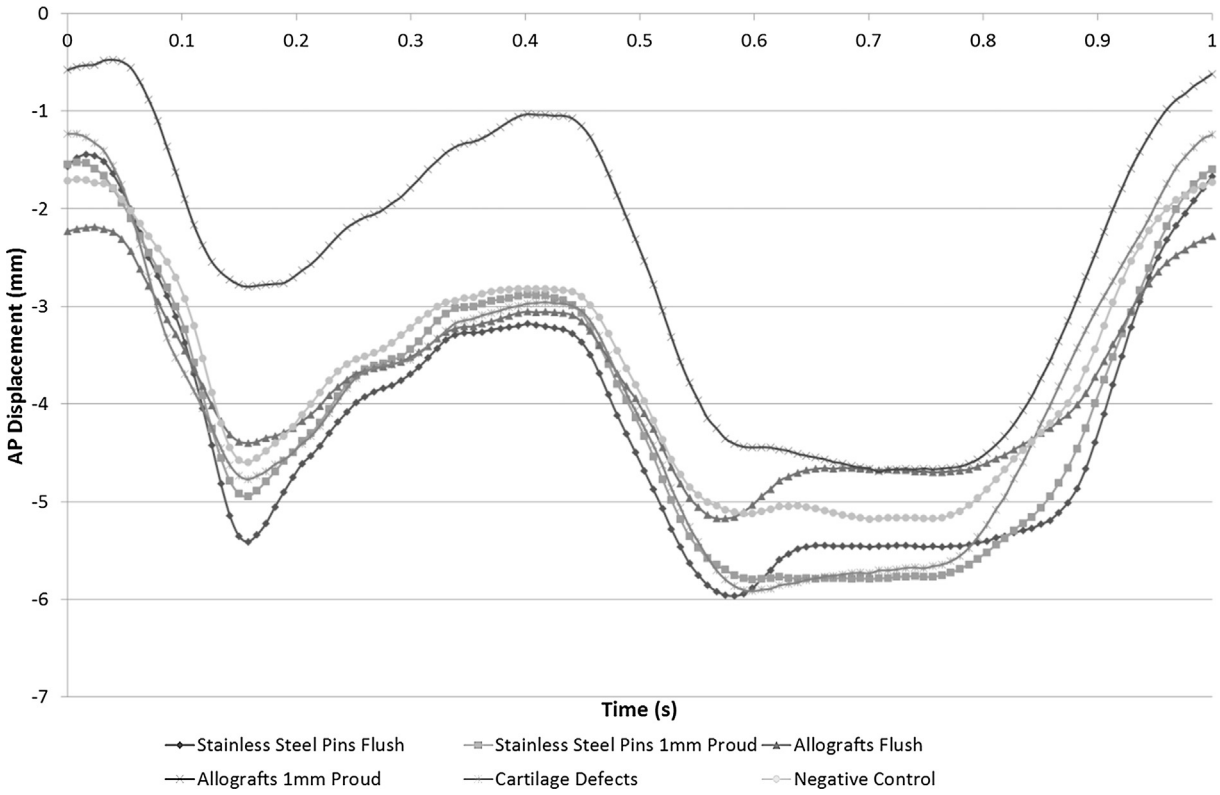


**Fig. 5.** Mean displacement values at 120 min test duration plotted against time during one cycle (1s) of the gait cycle (n = 4).

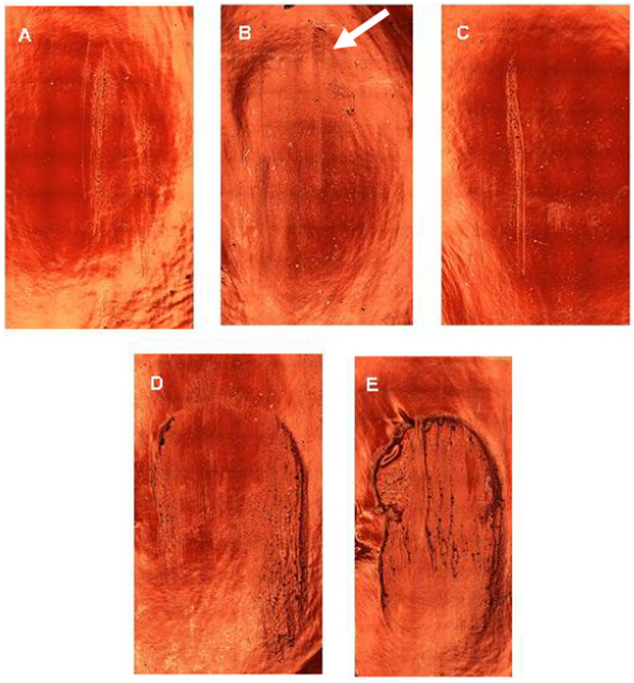


**Fig. 6.** Example Alicona Infinite Focus scan images of the meniscal surface replicas. Posterior towards the top of each image. (A) Allografts Flush Group; (B) Allografts 1 mm Proud Group (with arrow showing region of the hemispherical depression); (C) Cartilage Defects Group; (D) Positive Control Group 1 (Stainless Steel Pins Flush; (E) Positive Control Group 2 (Stainless Steel Pins 1 mm Proud).

0.009 mm), however, the difference was not significant ($p = 0.426$). No significant differences ($p = 0.992$) were present between the cartilage defect and allograft flush groups.

## 4. Discussion

It is important to determine the changes that occur in the tissues of the natural joint in the presence of cartilage defects and osteochondral allografts (current surgical intervention) and how these compare to novel interventions such as regenerative scaffolds and constructs. This is the first report of experimental simulation of early osteochondral repair interventions in a whole knee joint model that has quantified surface wear, deformation and damage.

In order to assess the performance of novel osteochondral repair interventions, it is important to firstly understand the baseline tribological performance of the natural joint under physiologically relevant conditions. In this model the whole joint cartilage-on-cartilage (negative controls) exhibited no wear, deformation or damage. The integrity of the cartilage structure was maintained due to the biphasic nature of cartilage that promotes high levels of interstitial fluid pressurisation, load support and fluid rehydration. However, when stainless steel grafts (positive controls) were implanted either flush or 1 mm proud of the surrounding surface, a significant level of wear, deformation and damage was observed and quantified on the opposing meniscal surface; demonstrating the ability of the model to detect quantifiable changes in the meniscal surface.

The smallest change in volume extending below the surface from the negative control was observed with the allografts flush group. This low level of wear, deformation and damage could be attributed to the restoration of the articular surface and some level of biphasic lubrication. The simulation model used within this study represented the natural joint in the immediate post-operative period following osteochondral allograft implantation prior to the ingrowth of fibrocartilage repair tissue and integration with the underlying subchondral bone. The implantation of allografts produced a discontinuous articulating surface and did

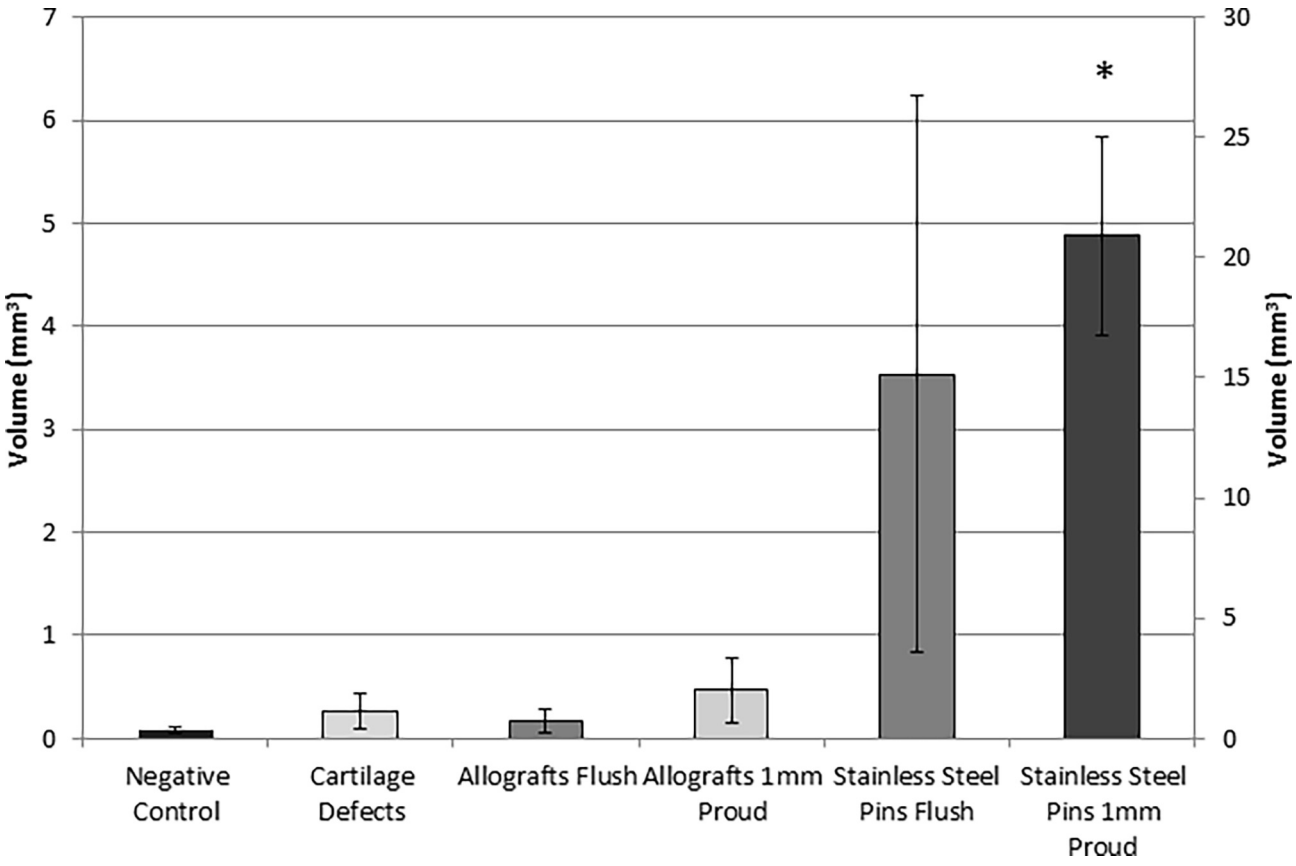


**Fig. 7.** Mean volume ($mm^3$) extending beneath the meniscal surface (mean ± 95% confidence intervals; n = 4 per group). For clarity, positive control group 2 (stainless steel pins 1 mm proud) has been plotted on the secondary axis. * indicates a significant difference ($p < 0.05$, ANOVA) in volume between the experimental group and negative control.

introduce the presence of edge effects. Studies have shown that the implantation of allografts into the femoral condyle can result in altered stress/strain distributions and contact pressures in the opposing cartilage surface, coupled with increased levels of friction when compared to the native joint (Wu et al., 2002; Lane et al., 2009; Bobrowitsch et al., 2014; McCann, 2009). Although, the insertion of allografts flush with the cartilage restored the articular surface, the effects of the aforementioned factors did result in a small volume of damage, wear and deformation.

A relatively low level of wear, deformation and damage was also observed in the cartilage defect group, however, different factors were thought to be at play when compared to the allograft group. These factors include for example, a reduced contact area, and increased fluid levels in the articulation increasing fluid support during the short duration of the experimental tests. Further, the appropriateness of the cartilage defect in terms of such a regular shape and depth for example, in relation to actual cartilage injuries observed clinically, needs to be considered and is perhaps a limitation of this study. Within the cartilage defect group, two of the four samples had extrusions on the tissue surface following testing; the approximate diameter of the extrusions (6 mm) was consistent with the diameter of the cartilage defect in the opposing femoral surface. The extrusions observed on the opposing meniscal surfaces were likely due to bulging of the meniscus into the cartilage defect under the compressive load, as also observed in previous small scale contact mechanics studies of focal articular defects (Gratz et al., 2009; Wong and Sah, 2010). These studies also noted a lateral expansion of the defect edges into the empty defect region; furthermore, with lateral motion, the opposing cartilage surface partially filling the defect, ploughed over and further compressed the edge of the cartilage defect while being compressed itself. It is anticipated that during longer test durations, and more appropriate replications of clinical cartilage injuries and defects, the level of wear, deformation and damage within the cartilage defect group would increase considerably due to the altered tissue mechanics.

There was a higher variation in the mean volume for the stainless steel grafts implanted flush; this was likely to be a reflection on how flush the grafts were – a lower volume of wear, deformation and damage may have occurred if the stainless steel pin had been recessed below the cartilage surface of the femoral condyle, hence reducing the contact between the hard bearing material and the meniscal surface. Overall, volumetric changes in surface geometry were adversely affected by grafts and stainless steel pins inserted proud of the cartilage surface, resulting in greater penetration depths. These higher resultant volumes of wear, deformation and damage with proud grafts, highlights the importance of surgical precision when implanting osteochondral allografts; and how this whole joint simulation model may be used to investigate variation in surgical precision and aid in the development of stratified interventions for the patient population. Previous studies have demonstrated the presence of abnormal contact tensile stresses in the tibial surface opposing proud allografts (Wu et al., 2002), similarly, allografts implanted 1 mm proud have been shown to significantly increase contact pressures up to 57% (Koh et al., 2004). Altered stress-strain distributions due to protruding grafts may predispose the joint surfaces to degenerative changes including softening and fibrillation of the cartilage tissue (Nakagawa et al., 2007).

Consistent patterns and locations of surface wear, deformation and damage were observed within each experimental group, indicating a good level of reproducibility in the method developed. Indeed, these results have shown the method developed and

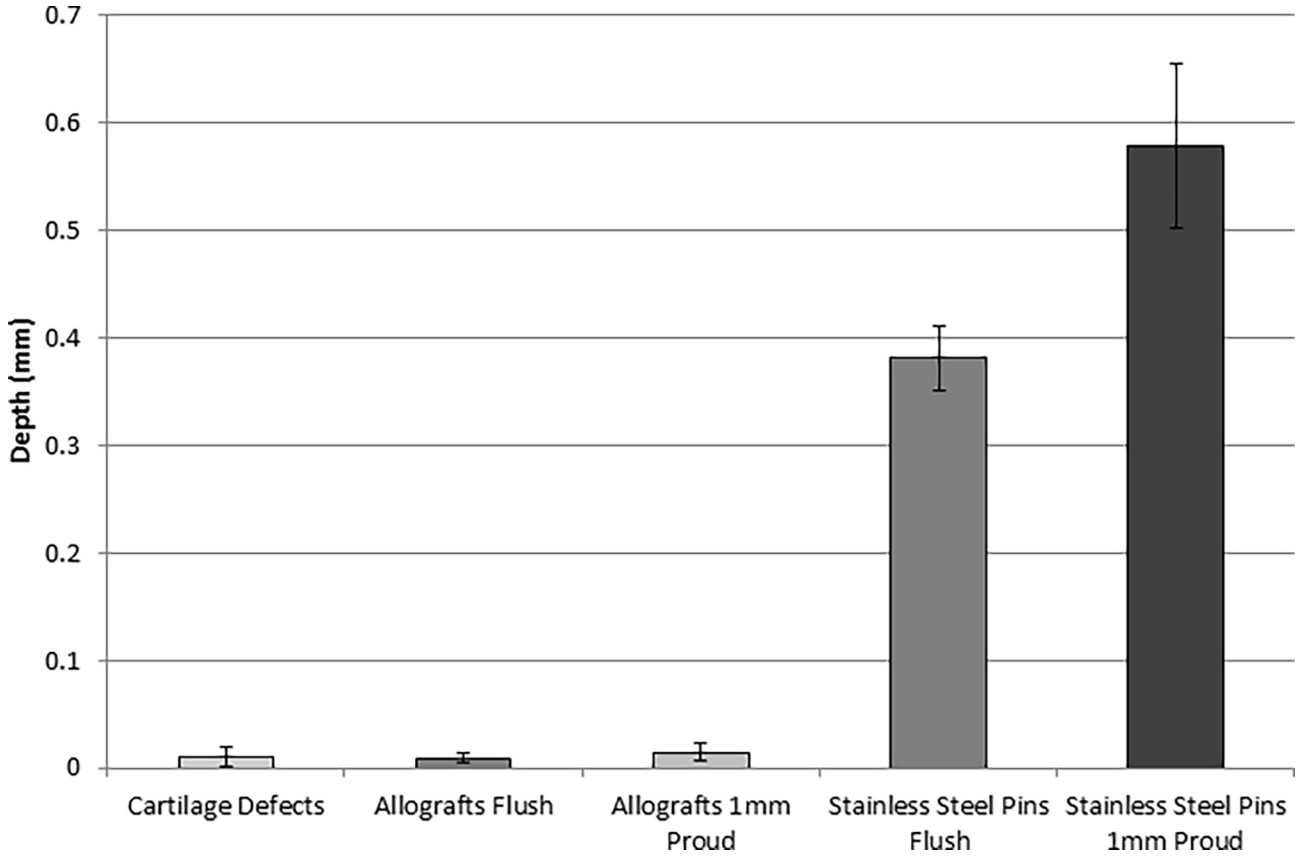


**Fig. 8.** Mean penetration depth measured in areas of damage, wear and deformation on the meniscal surface (mean ± 95% confidence intervals; n = 4 per group).

optical profilometry analysis technique to be sensitive enough to be able to quantify wear, deformation, damage, and discriminate between different interventions.

In terms of AP shear force and AP displacement all experimental groups exhibited similar trends at the end of testing with the exception of the allograft 1 mm proud group, which appeared to have a different offset for both AP shear force and AP displacement. However, it was clear that the AP shear force, used previously as a measure of friction (Liu et al., 2015), was not sensitive enough to discriminate between different interventions.

There were several limitations to this study. Firstly, the use of springs to constrain AP motion and replicate ligament function. Unfortunately it was not possible to retain the ligaments and perform the intervention, hence the use of springs to replicate ligament function. Secondly, the relatively short test duration was a limitation, and several findings from this study indicate that an increased test duration in future studies may facilitate a more robust assessment of tribological performance. Thirdly, the sample size of four per experimental group was a limitation, but was chosen based on the practicalities of the time involved in setting up and running the simulation studies, and the need to investigate 6 different experimental groups; despite the relatively small sample size the method was still able to discriminate between different interventions.

The method developed within this study may be applied in future work to a human joint model, however, the limitations of human donor tissue use, such as average donor age (70 years) (Dluzen et al., 1996; Cornwall et al., 2012; Sadhu et al., 2013), tissue quality and potential for established osteoarthritis must be taken into consideration when interpreting the results of tribological studies.

## 5. Conclusion

An *in vitro* method has been developed for the tribological evaluation of osteochondral grafts in a physiologically relevant whole joint simulation model of osteochondral defect repair. The development of the method facilitated the investigation of surface wear, deformation and damage in an *in vitro* whole joint simulator study for the first time.

## Acknowledgment

This research was funded by the EPSRC Doctoral Training Centre in Tissue Engineering and Regenerative Medicine, a collaboration between the Universities of Leeds, Sheffield and York. Grant number EP/500513/1. Research work on biotribology of cartilage at University of Leeds is supported by an EPSRC programme grant ('Optimising knee therapies through improved population stratification and precision of the intervention' EP/P001076/1) and ERC Advanced award REGENKNEE. John Fisher and Eileen Ingham are supported by the National Institute for Health Research (NIHR) Leeds Musculoskeletal Biomedical Research Centre and by the EPSRC Centre of Innovative Manufacturing for Medical Devices. The views expressed are those of the author(s) and not necessarily those of the NHS, the NIHR or the Department of Health.

## Declaration of conflicting interests

John Fisher and Eileen Ingham are consultants to Tissue Regenix and DePuy.

John Fisher and Eileen Ingham have equity holdings in Tissue Regenix.

John Fisher acts a consultant to Simulation Solutions and Invibio.

Research funding and support has been received by the University of Leeds in related areas in which the authors are directly involved as investigators from the following companies, Simulation Solutions, DePuySynthes, Invibio, Biocomposites, NHS Blood & Transplant, Mathys, Corin, MatOrtho.

## References

Bobrowitsch, E., Lorenz, A., Jorg, J., Leichtle, U.G., Wulker, N., Walter, C., 2014. Changes in dissipated energy and contact pressure after osteochondral graft transplantation. Med. Eng. Phys. 36 (9), 1156–1161.

Bowland, P., Ingham, E., Fisher, J., Jennings, L.M., 2018. Data Associated with 'Development of a Preclinical Natural Knee Simulation Model for the Biotribological Assessment of Osteochondral Grafts In Vitro. In: LEEDS, U.O. (Ed.), Leeds.

Bowland, P., 2016. Biotribology of Osteochondral Grafts in the Knee. University of Leeds (Ph.D thesis).

Bowland, P., Ingham, E., Jennings, L., Fisher, J., 2015. Review of the biomechanics and biotribology of osteochondral grafts used for surgical interventions in the knee. Proc. Inst. Mech. Eng. Part H-J. Eng. Med. 229 (12), 879–888.

Chu, C., Szczodry, M., Bruno, S., 2010. Animal models for cartilage regneration and repair. Tissue Eng. 16 (1), 105–115.

Cornwall, J., Perry, G., Louw, G., Stringer, M., 2012. Who donates their body to science? an international multicenter, prospective study. Anatomical Sci. Educ. 5 (4), 208–216.

Dluzen, D., Brammer, C., Bernard, J., Keyser, M., 1996. Survey of cadaveric donors to a body donation program: 1978–1993. Clin. Anat. 9 (3), 183–192.

Gratz, K.R., Wong, B.L., Bae, W.C., Sah, R.L., 2009. The effects of focal articular defects on cartilage contact mechanics. J. Orthop. Res. 27 (5), 584–592.

Koh, J.L., Wirsing, K., Lautenschlager, E., Zhang, L.O., 2004. The effect of graft height mismatch on contact pressure following osteochondral grafting: a biomechanical study. Am. J. Sports Med. 32 (2), 317–320.

Lane, J., Healey, R., Amiel, D., 2009. Changes in condylar coefficient of friction after osteochondral graft transplantation and modulation with hyaluronan. Arthroscopy 25 (12), 1401–1407.

Liu, A., Jennings, L.M., Ingham, E., Fisher, J., 2015. Tribology studies of the natural knee using an animal model in a new whole joint natural knee simulator. J. Biomech. 48 (12), 3004–3011.

Mccann, L., 2009. Tribological Investigation of Articular Cartilage Substitution in the Medial Compartmental Knee. University of Leeds (Doctor of Philosophy thesis).

Mccann, L., Udofia, I., Graindorge, S., Ingham, E., Jin, Z., Fisher, J., 2008. Tribological testing of articular cartilage of the medial compartment of the knee using a friction simulator. Tribol. Int. 41, 1126–1133.

McEwen, H.M.J., Barnett, P.I., Bell, C.J., Farrar, R., Auger, D.D., Stone, M.H., Fisher, J., 2005. The influence of design, materials and kinematics on the in vitro wear of total knee replacements. J. Biomech. 38, 357–365.

Nakagawa, Y., Suzuki, T., Kuroki, H., Kobayashi, M., Okamoto, Y., Nakamura, T., 2007. The effect of surface incongruity of grafted plugs in osteochondral grafting: a report of five cases. Knee. Surg. Sports Traumatol. Arthrosc. 15 (5), 591–596.

Sadhu, A., Meyer, R., Kundu, B., Biswas, S., Chakraborty, S., 2013. Trends in body donation for medical education: 10 year retrospective study. Ind. J. Basic Appl. Med. Res. 2 (8), 1089–1092.

Wong, B.L., Sah, R.L., 2010. Effect of a focal articular defect on cartilage deformation during patello-femoral articulation. J. Orthop. Res. 28 (12), 1554–1561.

Wu, J., Herzog, W., Hasler, E., 2002. Inadequate placement of osteochondral plugs may induce abnormal stress-strain distributions in articular cartilage-finite element simulations. Med. Eng. Phys. 24 (2), 85–97.